S

Space Radiation Shielding

Cary Zeitlin
Leidos Innovations Corporation, Houston, TX, USA

Contents

Definition

Both short- and long-term health risks from exposure to galactic cosmic rays (GCRs) and solar energetic particles (SEPs) are potentially limiting factors in the human exploration of deep space. A significant portion of the risk is attributable to the presence of high-energy heavy ions in space, particles that do not exist on the surface of the Earth and which are known to cause biological damage disproportionate to the physical dose they impart. Large uncertainties remain in our knowledge of the biological effects of high-energy heavy ions, particularly at the low dose rates encountered in space (Cucinotta 2015).

In conventional radiation protection, three principles apply: (1) minimize the duration of the exposure; (2) maximize the distance from the source; (3) place shielding between personnel and the source whenever possible. In space, the first two principles cannot be readily applied, and the utility of shielding is severely limited by the high cost of launch and by the fact that many GCRs have high energies and cannot be stopped by practical shielding depths. There are scenarios in which SEPs can be a major concern, but typically they can be shielded by conventional means, and the GCRs are more problematic for planning long-duration missions into deep space.

The value of shielding must be evaluated in terms of quantifiable effects. At first glance, this may seem to be a trivial statement, but the questions of exactly which effects are relevant, and how to evaluate them, have no definitive answers at present. This inherent uncertainty has spawned varying approaches to radiation protection of astronauts by the world's space agencies. The underlying problem is estimation of risk to a small population of healthy individuals that receive radiation doses that are far lower (and

L. R. Young, J. P. Sutton (eds.), *Encyclopedia of Bioastronautics*,
https://doi.org/10.1007/978-3-319-10152-1_28-1

accumulated at a far lower rate) than the doses received by the cohort of atomic bomb survivors in Japan or by cancer patients who have received radiation therapy. Risk estimates must be obtained by extrapolation, typically using the linear no-threshold (LNT) model, which in itself is controversial. In contrast, it is comparatively straightforward to study the effect of shielding on physical dose (energy deposited per unit mass, SI unit of J kg^{-1}, denoted by Gray, abbreviated as Gy), or on dose equivalent, which is the dose modified by a relatively simple biological effectiveness weighting function (SI unit of Sievert, or Sv). Dose equivalent can be used to estimate the likelihood for cancer induction for terrestrial exposures, but whether it accurately describes the cancer risk from exposure to space radiation is an open question. Nonetheless, for the sake of simplicity in evaluation shielding questions, dose and dose equivalent are used here. The more complicated analyses that are necessary for detailed risk estimations could conceivably lead to conclusions about shielding effectiveness that differ from those reached by studying dose and dose equivalent. Furthermore, the physics transport models that are used to predict details of the radiation field at points inside a shielded vehicle and an astronaut's body are in a constant state of development and subject to significant change over time as models improve.

Measurements and calculations of dose and dose equivalent depend on knowledge of the linear energy transfer (LET) spectrum in water that is present in the radiation environment of interest. LET is closely tied to the concept of ionization energy loss, or dE/dx, which is discussed in detail below. Dose is obtained by integrating over the LET spectrum; dose equivalent is obtained by integrating the LET spectrum weighted by a biological response function referred to as the quality factor (ICRP 1991). Typical terrestrial sources of radiation (other than radon) have low LET. Space radiation contains both low- and high-LET components.

Detailed Description

The three principles of radiation protection are difficult or impractical to apply to human spaceflight. First, because radiation dose rates are generally far too low to cause acute effects, mission durations have to date been driven by other considerations, more or less rendering the first principle inoperable. The second principle does not apply in space, because the sources are omnipresent: GCRs impinge from all directions, as do SEPs, except in the early stages of a solar event. This leaves only the third principle, shielding, as a possible means of mitigating exposures. Many approaches to the shielding problem have been suggested, including active shields using magnetic or electrostatic fields. Unfortunately, the high cost of launch, coupled with the high energies of GCRs, makes shielding against them by either active or passive methods highly problematic. Shielding is far more effective against SEPs, and in typical solar events, even modest depths can reduce exposures to acceptable levels owing to the generally low energies of the particles compared to GCRs. We begin by describing the sources of energetic particle radiation in space, followed by an overview of the physical processes relevant to transport of these particles through matter. We then discuss approaches to shielding, both "bulk" and active, highlighting the difficulties associated with all current technologies. Throughout, it is helpful to make use of existing calculational tools to illustrate the complex interplay of the physical effects that influence shielding. Those used here include:

- The Badhwar-O'Neill GCR Flux Model (O'Neill et al. 2015.
- The Proton Stopping-Power & Range Tables database, PSTAR (Berger 1992)
- The Particle and Heavy Ion Transport System (PHITS), a Monte Carlo simulation code (Niita et al. 2006.
- The Online Tool for the Assessment of Radiation in Space, OLTARIS (Singleterry 2011)

Aside from the PSTAR database, none of these tools is unique for its application, and their use

here is a matter of convenience and does not constitute an endorsement. One could just as well use, e.g., the Nymmik et al. model of GCR fluxes (Nymmik et al. 1996), the GEANT4 Monte Carlo package (Agostinelli et al. 2003), among other choices, and the conclusions reached would be similar if not identical.

In describing the kinetic energies of particles in the space radiation environment, it is convenient to use units of mega-electron volts (MeV) for protons and MeV/nucleon or MeV/nuc for heavier ions. Since a hydrogen nucleus consists of a single nucleon (a proton), the terms are interchangeable when discussing these particles.

Sources of Energetic Particles in Space

In deep space, the galactic cosmic rays are a continuous, low-level source of radiation exposure, and solar energetic particles are a sporadic, potentially high-level source. In low-Earth orbit (LEO), there is a third component, energetic protons and electrons in the South Atlantic Anomaly (SAA), a region of trapped particles through which orbiting spacecraft fly a few times per day. The SAA is not a concern for deep space missions, but traversal of the more intense outer belts of trapped particles is of some concern.

GCRs and the Solar Cycle

The origin of cosmic rays has been debated since their discovery over 100 years ago (Hess 1913). An excellent recent review was written by Blasi (2013). A full understanding of the mechanism or mechanisms by which GCRs are accelerated continues to be elusive. As the name implies, GCRs are produced within the Milky Way galaxy, not in the solar system, and can enter the heliosphere if they possess enough energy to overcome the barrier posed by the Sun's "magnetic bubble," which extends to at least 120 AU (Stone et al. 2013). There is now strong observational evidence that cosmic ray acceleration largely occurs in supernova remnants through diffusive shock acceleration (Baade and Zwicky 1934). The accelerated particles then undergo diffusive transport in the galactic magnetic field. The spectrum of GCRs that impinges on the heliosphere is referred to as the "LIS" for local interstellar spectrum. GCRs in the LIS are diffusively transported through the heliosphere, under conditions that vary significantly throughout the course of the approximately 11-year solar cycle. At solar maximum, when the solar magnetic field is strongest, low-energy GCRs do not reach the inner heliosphere; conversely, at solar minimum, lower-energy ions are able to penetrate.

Solar activity, which has its visible manifestation in the form of sunspots, is linked to the strength of the interplanetary magnetic field (IMF), which determines the potential barrier presented to incident GCRs in the LIS. Sunspots have been observed for over 400 years, and the cyclic nature of solar activity was noted more than 170 years ago (Schwabe 1844). Several excellent reviews of the current state of knowledge of the solar cycle can be found in the literature (Hathaway 2010; Charbonneau 2014). There is general agreement that dynamo processes drive the cycle, but, as in the case of GCR acceleration mechanisms, our understanding of the fundamental physics is incomplete. This knowledge deficit precludes accurate long-term prediction of solar activity and consequently makes long-term predictions of GCR modulation unreliable.

Despite the existing knowledge gaps, much is known about the GCRs, and the high-energy portion of the spectrum (kinetic energies above 1–2 GeV/nuc) is much less affected by solar modulation than is the low-energy portion. High-energy GCR ions present the greatest – possibly insurmountable – challenges to any shielding method. The difficulty of the problem can be gleaned from Fig. 1, which shows cumulative distribution functions (CDFs) as functions of energy for protons and helium under solar minimum and solar maximum conditions. Protons comprise about 88% of GCRs, and helium ions about 10% of GCRs. These two types of ions are dominantly low-LET sources. Fluxes were calculated using the 2014 version of the Badhwar-O'Neill GCR model (O'Neill et al. 2015). The remaining 2% of the GCR flux is approximately equally divided between electrons and heavy ions, that is, those with charge $Z > 2$. The latter are the source of high-LET radiation in space, and it is the exposure to this high-LET radiation that presents

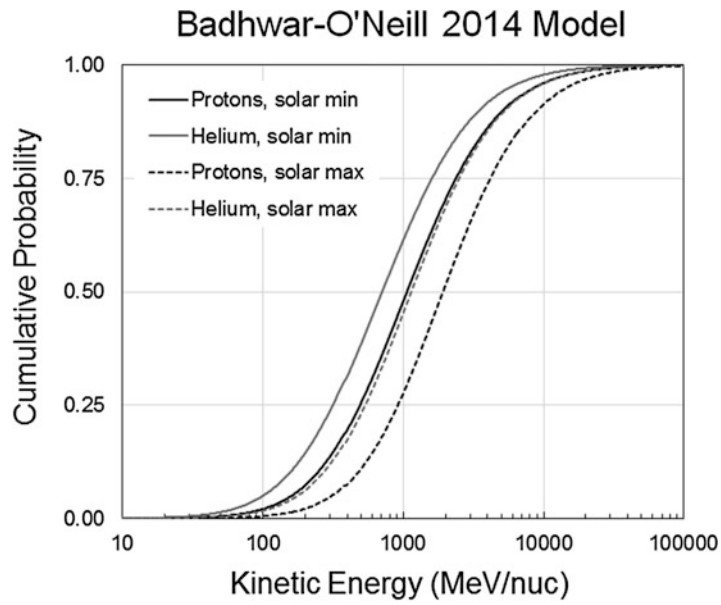

Space Radiation Shielding, Fig. 1 Model calculations of cumulative probability distributions for protons and helium ions in the galactic cosmic rays, at solar minimum and solar maximum

the greatest uncertainty in assessment of health effects.

CDFs are a useful way to look at GCR spectra in the context of shielding, as the distributions can be used in combination with the range-energy relation (given below) to easily determine the fractions of particles that might be stopped in various shielding scenarios. Note that under solar maximum conditions, about half of GCR protons have energies above 1 GeV. At solar minimum, the 50% point of the distribution is reached at about 700 MeV. The helium CDF at solar maximum is remarkably similar to that for protons at solar minimum; here again the 50% point is reached at about 1 GeV/nuc, whereas at solar maximum, it is reached at about 1.7 GeV/nuc.

The intensity of GCRs in unshielded interplanetary space is largest at solar minimum; in the recent deep minimum of 2009–2010, the rate of protons and helium with energies above 180 MeV/nuc was about 6 cm^{-2} s^{-1}. During a typical solar maximum, the comparable rate is suppressed, to about 2 cm^{-2} s^{-1}. Corresponding dose rates in tissue are moderate, about 500 microGy/day (5×10^{-4} Gy) at solar minimum and about 160 microGy/day for a typical solar maximum. The solar minimum estimate is consistent with results obtained by the MSL-RAD detector during the Curiosity rover's transit from Earth to Mars in 2011–2012 (Zeitlin et al. 2013a). This is about a factor of 600 greater than the annual cosmic ray background dose rate at sea level on Earth but orders of magnitude less than the rate at which acute health effects begin to be seen (when doses of at least 0.7 Gy are received, typically over a span of minutes). It is well known that subacute radiation exposures cause an increase in cancer rates, but health effects of chronic low dose rates are extremely difficult to assess (Brenner et al. 2003).

SEPs

Solar energetic particles are produced by the Sun sporadically, with events occurring most often at or near solar maximum. Compared to GCRs, SEPs have low energies, typically below 100 MeV/nuc. SEPs also typically have a lower abundance of heavier ions than do GCRs. Rare events with significant fluxes of high-energy ions have been observed (Tylka and Dietrich 1999), but usually SEP spectra are "soft," that is, the flux distributions peak at low energies, with modest or negligible fluxes at energies of concern for astronauts in a vehicle or habitat. However, very large particle fluxes of low-energy ions can be a concern for astronauts when they are in lightly

shielded environments, for example, when doing an extravehicular activity (EVA) far from shelter.

Our knowledge of SEP events is mostly derived from data obtained since the start of the Space Age, when particle detectors began to be launched into orbit to measure particles and fields in the vicinity of Earth. One notable exception to this is the Carrington Event of 1859 (Cliver and Dietrich 2013; Smart et al. 2006). R.C. Carrington, a British amateur astronomer, was making observations of sunspots when he observed a brilliant but short-lived white-light solar flare. The Coronal Mass Ejections (CME) associated with the flare was extremely fast, and reached Earth within 17 h, causing a huge geomagnetic storm that was (eventually) the first to be understood as having its origin in solar activity. Of course, no measurements of either primary or secondary particle fluxes were possible at the time, and determination of such fluxes from ice cores is highly uncertain (Wolff et al. 2012). Nonetheless, the Carrington Event is sometimes considered a worst-case scenario for SEP events (Townsend et al. 2006), with particle fluxes possibly high enough to cause acute health effects, depending on assumptions about the energy spectrum (Stephens et al. 2005).

EVA Exposures

Although SEP events typically do not produce enough high-energy particles to be a concern for a reasonably well-shielded crew, there are scenarios in which large exposures from SEPs are possible. Of these, a highly plausible case would be astronauts performing a sortie on the lunar surface, in which they drive a rover to a destination several hours away from the main habitat. For the most part, even in such an exposed situation, enough time elapses between the onset of a SEP event and the arrival of particles at 1 AU that there is sufficient time to reach shelter (Reames 1999). However, in January 2005 an intense SEP event occurred in which less than an hour elapsed between a solar flare and the arrival of flare-accelerated particles at 1 AU (Mewaldt et al. 2005). The observation of such an event shows that a portable shelter of some sort will be required for such sorties.

SAA

The South Atlantic Anomaly (SAA) is a region centered near the east coast of Brazil where the Earth's inner trapped particle belt dips to its lowest altitude. Spacecraft in low-Earth orbit (LEO) may pass through the SAA several times per day, during which time dose rates are observed to rise dramatically (Reitz et al. 2005), even inside relatively well-shielded vehicles such as the International Space Station (ISS). Roughly half the accumulated dose received by astronauts on the ISS is attributable to SAA passes. The dose in the SAA is due to protons and electrons (low LET), and inside a shielded vehicle, to secondary neutrons produced by the trapped protons. The large majority of trapped protons in the SAA have energies below 100 MeV, similar to typical SEP distributions.

Shielding Physics Overview

Evaluating the effects of shielding is based on comparison of the radiation fields "before" and "after" the shield. Ideally, a shield would allow for no "after" particles, i.e., every incident particle would be stopped or otherwise absorbed in the shield. This is feasible with very low-energy laboratory sources such as alpha or beta emitters. In scenarios involving more energetic particles, such as at terrestrial particle accelerators, shielding is designed so that all incident charged particles are stopped, and though secondary radiation emerges from the shield, it is far less intense and less harmful than the incident particles. Unfortunately, in space, neither of these cases is realizable in practice: some or much of the primary GCR radiation will penetrate any practical depth of shielding, and sometimes interactions make the radiation emerging from the shield more biologically effective than the primary particle was. For SEPs and most trapped particles, conventional notions of shielding against these particles by stopping them can be applied effectively, because energies and hence ranges are modest.

Electromagnetic Interactions: dE/dx and the Range-Energy Relation

For purposes of assessing health risks to crewmembers, the threshold for defining an

"energetic" charged particle can be considered to be the energy at which a particle has sufficient range to penetrate the most minimal shielding an astronaut might be under. We are therefore concerned with the fundamental relation between a particle's energy and its range in matter, i.e., the range-energy relation. This can be derived from integration of the differential energy loss equation first developed by Bethe (Bethe 1930). The original Bethe equation, which describes ionization energy loss – that is, the electromagnetic interaction between a charged particle and the atomic electrons of the medium is traversing – has been further refined to yield a formalism that is accurate to roughly 1% over a large span of particle energies and types (Olive et al. 2014).The change in energy of a charged particle, dE, traversing an infinitesimal depth of matter, dx is given by:

$$\frac{dE}{dx} = -k\rho\left(\frac{Z}{A}\right)_{mat}\left(\frac{Z}{\beta}\right)^2_{proj}\left[\log\left(\frac{2m_e\beta^2}{I\left(1-\beta^2\right)}\right)-\beta^2\right]$$

where k is a constant, Z refers to atomic number, A to mass number, β is the velocity of the moving particle relative to the speed of light, I is the ionization potential of the medium, and ρ its density. The subscript "mat" refers to the material being traversed (often referred to as the target, here as the shield), while "proj" refers to the projectile, that is, the energetic particle that is losing energy. It is sometimes helpful to consider the term in brackets to be approximately constant or at least slowly varying with projectile energy; though crude, this approximation sheds light on the fundamental dependence of energy loss on the charge and velocity of the projectile (Z^2/β^2) and on the charge to mass ratio of the target material $(Z/A)_{mat}$. Integration of the dE/dx versus energy curve yields the range-energy relation for any given combination of projectile and target. To a very good approximation, the proton range for a given energy and material can be scaled to obtain the range of an ion with the same velocity (or energy per nucleon) having charge Z and mass number A according to (A/Z^2). This means that ^{4}He ions have almost exactly the same range as protons for the same energy per nucleon.

The range-energy relation is crucially important when considering shielding against the space radiation environment. In some cases, charged particles can be shielded against by "ranging them out," that is, by providing a sufficient depth of shielding mass that the particles lose all their kinetic energy in the shielding before reaching a biological target. For example, alpha particles emitted by radioactive nuclei have typical energies of a few MeV and generally can be stopped by a single sheet of paper. In contrast, a proton with kinetic energy of 1 GeV (roughly the average for GCRs) has a range exceeding 1.5 m (greater than 400 g cm^{-2}) in aluminum. For purposes of radiation protection of humans in space, it is necessary to consider what particles might penetrate the thinnest portion of a spacesuit, which is the only protection for an astronaut performing an EVA, including sorties on the lunar surface. The thinnest part of the Enhanced Mobility Unit used on the ISS is about 0.2 g cm^{-2} or 0.74 mm (Moyers et al. 2006); the energy for a proton to penetrate this depth is about 15 MeV, and electrons with energies above about 500 keV can also penetrate this depth. These energies are orders of magnitude greater than the energies of solar wind particles, so that source can be dismissed from consideration of health risks to astronauts. However, virtually all GCRs and many SEPs have sufficient energy to penetrate this part of the space suit. A more typical situation might be inside a thin-hulled spacecraft, with shielding on the order of 10 g cm^{-2} of aluminum (about 4 cm) interposed between the crew and free space; this depth is sufficient to stop a 100 MeV proton and therefore provides protection against most SEPs and a small fraction of GCRs.

The energy dependences of dE/dx (left) and range (right) are shown in Fig. 2 for protons in aluminum. The calculations were made using the PSTAR program, which is available on a public website maintained by the US National Institute of Standards and Technology (http://physics.nist.gov/PhysRefData/Star/Text/PSTAR.html). The steeply rising portion of the dE/dx curve below about 300 MeV is sometimes referred to as the

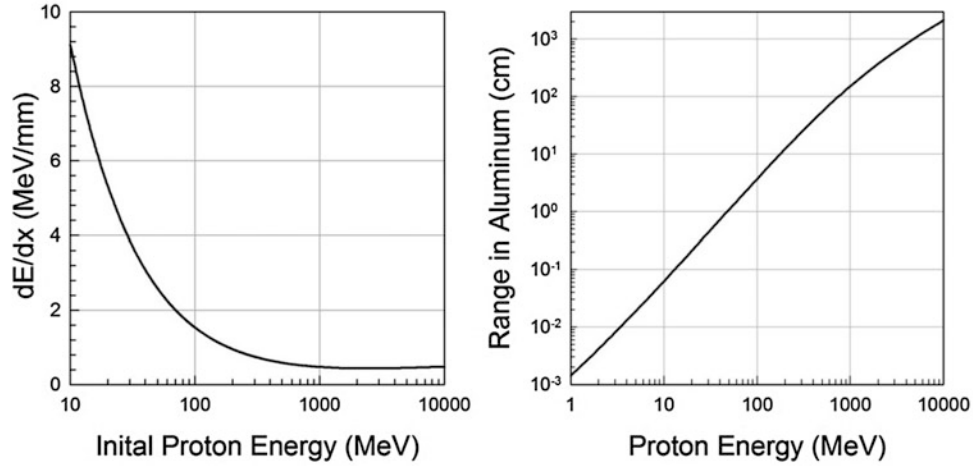

Space Radiation Shielding, Fig. 2 Calculations of proton energy loss (left) and range (right) in aluminum, made using the NIST PSTAR database

"one over beta squared" region. This is where particles can readily be stopped in modest depths of material, because of the rapid increase of dE/dx with penetration depth. At higher energy, in the relatively flat portion of the curve, dE/dx remains nearly constant with increasing depth. Put another way, highly energetic particles have a more or less constant rate of slowing down in a shield, and this rate is insufficient to stop the large majority of GCRs.

The graphs in Fig. 2 should be evaluated in conjunction with Fig. 1, which shows that the GCR environment consists mostly of protons and helium ions with energies above a few hundred MeV/nuc. Taken together, the implication is clear – even a substantial shield consisting of 10 cm of aluminum (27 g cm^{-2}) would not be enough to stop the large majority of these ions, even at solar minimum. To stop even half the proton flux at solar maximum would require a full meter depth of aluminum, which is clearly impractical. Another way to look at this relation is to consider the fraction of energy a particle loses in traversing a given depth of material. Figure 3 shows the fractions lost by protons in aluminum and water. Water is included in the comparison because it is hydrogenous, and, for reasons that will become clear in the discussion of nuclear interactions, hydrogenous shields are expected to be highly effective shields against GCR heavy ions. The curves in Fig. 3 show that hydrogen is slightly more effective in stopping particles than is aluminum, per unit areal density. But even with this more effective material, stopping protons or helium ions with energies above a few hundred MeV/nuc requires many tens of (g cm^{-2}) of material, the same conclusion one would reach based on dE/dx in aluminum.

Nuclear Interactions

Electromagnetic interactions are extremely important in shielding, as described in the preceding section. These interactions are well understood from both the theoretical and experimental perspectives. Nuclear interactions are equally important but are, however, not nearly as well understood from the theoretical perspective. Electromagnetic interactions between a projectile and the surrounding medium are dominantly due to interactions with the atomic electrons of the medium and are described by quantum electrodynamics (QED), which has proven to be extremely accurate. Nuclear interactions are, in contrast, collisions between the projectile and a nucleus in the medium. All of the participating particles contain smaller constituents (nuclei contain nucleons, and nucleons contain quarks and gluons). From the perspective of space radiation shielding, the most important nuclear interactions are proton-nucleus and nucleus-nucleus collisions. Because

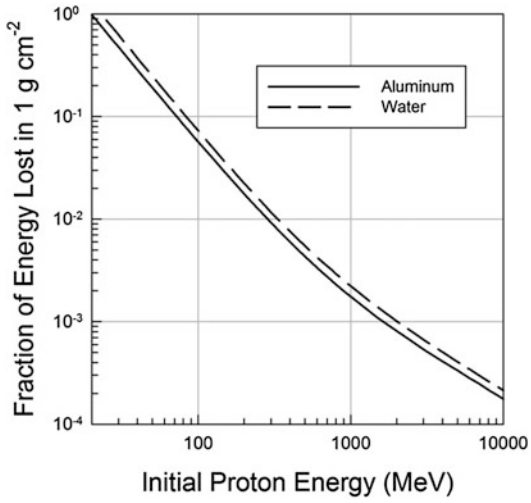

Space Radiation Shielding, Fig. 3 Fraction of initial energy lost by protons in 1 g cm^{-2} of material, calculated for aluminum and water using the NIST PSTAR database

the fundamental particles involved are quarks and gluons, one might hope that quantum chromodynamics (QCD) could describe their interactions with accuracy comparable to that with which QED describes electromagnetic interactions. However, nucleons are bound states of quarks and therefore exist in the "non-perturbative" energy domain in which QCD calculations are highly problematic. There is, accordingly, no fundamental theory that describes these interactions from first principles, though work is ongoing in this field (Detmold 2015). In the absence of a fundamental theory, nuclear physicists have developed semiempirical models which are incorporated into various Monte Carlo simulation packages, with varying degrees of accuracy (Sihver et al. 2007; Ronningen et al. 2013; Oh et al. 2015).

Electromagnetic interactions are dominantly elastic collisions, that is, collisions in which energy is transferred from one particle to another, but the incoming particles retain their identities. Nuclear interactions may also be elastic, but inelastic collisions dominate at high energies and are critical in space radiation shielding. Inelastic collisions produce secondary radiation that may have significantly different potential for causing biological damage than the incident radiation. The alteration of the radiation environment can go in either direction, that is, the secondary radiation may be less damaging than the primary, or it may be more damaging, depending on the details of the incident flux and the shield.

In the context of space radiation shielding, there are two main cases to consider within the broad category of nuclear interactions, proton-nucleus collisions and nucleus-nucleus collisions. In this context, "nucleus" refers to all elements other than hydrogen on the periodic chart, i.e., helium and heavier nuclei. The effects of nuclear interactions on the radiation environment behind shielding are very different for the two cases: proton-nucleus collisions tend to make the environment behind the shield more hazardous (Cucinotta et al. 1991), whereas nucleus-nucleus collisions tend to do the opposite.

Proton-Nucleus Collisions

Protons may collide with nuclei in the medium, with a variety of outcomes, probabilities which depend upon the projectile energy and the composition of the target material. The simplest case is a proton traversing hydrogen, so that only proton-proton collisions occur. Even in this case, secondary particle production is possible if the energy of the incident proton is large enough. In the framework of considering "before" and "after" radiation, consider a case in which an incident high-energy proton (with, say, 1 GeV or greater kinetic energy) collides with a nucleus. Even if the interaction is peripheral (that is, a grazing collision), significant energy can be transferred from the projectile to the target, so that one or more nucleons are removed from the target nucleus. Thus the "after" radiation consists of the initial energetic proton along with one or more nucleons removed from the target. Compared to the situation that would have existed had there been no collision, the shield has made the radiation environment worse. Furthermore, for sufficiently energetic protons, charged and neutral pions may be created, and these particles (or their decay products) can have enough energy to pass through the remaining depth of the shield.

It is generally the case for incident protons that secondary production makes the "after" dose

greater than the "before" dose, regardless of the shielding material, assuming that the proton energies are high enough and the shield is not so thick that it stops a large share of the incident protons. This is the result of inelastic collisions in which it is possible to produce secondary particles, in some cases large numbers of them. Some of these may be "knockouts," while others are "target fragments," that is, low-energy particles released when the struck nucleus, excited by the collision, decays to a ground state via emission of nucleons. A charged target fragment such as a proton or helium nucleus will typically have high LET and a short range due to the low kinetic energy imparted in the decay process and as a result may not leave the shield. Nonetheless, such particles may be locally damaging, particularly when produced inside a biological target. In some scenarios, the contribution of target fragments from interactions occurring inside an astronaut's body may account for up to half the equivalent dose (Cucinotta et al. 2006).

Target fragments may include neutrons, which can leave the shield even if their energies are low (~1 MeV), since they do not lose energy via dE/dx. Neutrons are thus able to penetrate to inhabited regions of a vehicle, where they become part of the complicated radiation field to which astronauts are exposed. Neutrons are capable of penetrating large depths of matter and can deliver a dose to tissue in the form of high-LET recoil protons.

Results from simulations of water and aluminum shields of 10 g cm^{-2} depth are shown in Table 1 to illustrate these effects. The Particle and Heavy Ion Transport System (PHITS) Monte Carlo code (Niita et al. 2006) was used with geometry similar to a particle beam experiment, with a pencil beam of monoenergetic protons of various energies entering the shields. The doses due to particles before and after the target were computed, and the ratios are shown for the two shield materials. These calculations are meant to be illustrative and are by no means definitive given the relatively small samples that were generated. The two important points are that the dose behind shielding is invariably greater than the dose before it, for these energies (all of which are sufficient to penetrate 10 g cm^{-2}), and that the ratio increases with increasing proton energy due to enhanced secondary production. At high energies, the ratios behind the aluminum shield are higher than those behind the water shield. Given that GCRs are mostly protons and that a large share has energy above 1 GeV, the inherent difficulty of the shielding problem starts to become clear from these considerations.

In summary, nuclear interactions between a proton and a nucleus in a shield generally result in a worsening of the environment inside the shield compared to the case where the incident proton passed through the shield without interacting. The increase in dose behind the shield is a strong function of the incident proton energy, but at typical GCR energies, even a few tens of (g cm^{-2}) of shielding depth tends to have a deleterious effect. Similar concerns arise in the area of proton therapy for cancer treatment (Paganetti 2002).

Nucleus-Nucleus Collisions

Incident nuclei with $Z > 1$ may also undergo nuclear interactions as they traverse a shield. Even though the interactions may, like proton-nucleus collisions, produce a large number of secondary particles, shielding generally reduces the hazard from heavy ions due to the effects of nuclear fragmentation. Although heavy ions represent only about 1% of the GCR flux, their contribution to dose in unshielded space can be on the order of 50%. This disproportionate contribution can be understood by examining the Bethe equation above, noting that the energy loss (which is directly related to dose imparted) is proportional to Z^2, that is, to the square of the projectile's charge. This simple scaling can be used to roughly estimate relative shares of dose; e.g., though protons are about eight times more abundant than helium ions, the latter are four times more ionizing, so the dose from protons is roughly twice as large as that from helium ions. Similarly, the flux of C, N, and O ions combined is about a factor of 15 less than that of He, but the dose per ion is about ten times larger for the heavier ions, thus their combined dose contribution is about two-thirds as large as that from helium.

Space Radiation Shielding, Table 1 Proton beam simulations with 10 g cm^{-2} Shields

Proton energy (MeV)	Dose after/dose before aluminum target	Dose after/dose before water target
500	1.07	1.11
1000	1.17	1.17
3000	1.48	1.29
5000	1.38	1.27

In nuclear fragmentation, one or more nucleons are stripped from the projectile, yielding fragments that continue with approximately the same direction and velocity as the incident ion. For a flux of highly energetic ions incident on a thin shield, where the incident ions are not significantly slowed by dE/dx, the dose behind the shield will be less than that incident on the shield. This is driven by the Z^2 dependence of dE/dx; to take a simple example, consider an incident high-energy carbon ion ($Z = 6$) that undergoes a peripheral collision with a nucleus in the shield and breaks into a boron ion ($Z = 5$) and a proton. The incident ion imparts a dose proportional to $Z^2 = 36$, while the fragments impart a dose proportional to the sum of the squares of the charges, which in this case is 26. Relative to the incident dose, the dose seen behind the shield is thus (26/36), or 72%, as large. Given that the dose from GCR heavy ions is roughly half of the total dose and that nuclear fragmentation cross sections are relatively large, this mechanism provides an achievable means of reducing the dose contribution from heavy ions, at the expense of an increased flux of light ions (protons, helium, etc.) and neutrons.

The probability for nucleus-nucleus collisions is well described by a simple geometric approximation in which the projectile and target nuclei are treated as overlapping spheres. The energy-independent geometric cross-sectional formula first proposed by Bradt and Peters (1950) and later modified by Townsend and Wilson (1986) describes these interactions with reasonable accuracy and a minimal number of free parameters over a wide range of projectiles, targets, and energies. Given the cross section (σ) for a particular interaction, the probability of its occurrence in a shield of depth x is given simply by $\exp(-x/\lambda)$ where λ is the mean free path, related to the cross section by:

$$\lambda = \frac{A}{N_A \sigma}$$

where A is the mass number of the shield material and N_A is Avogadro's number. A numerical example may be helpful. Consider a high-energy GCR silicon ion ($Z = 14$, $A = 28$) incident on an aluminum shield. The Wilson et al. cross-sectional formula predicts a charge-changing cross section of 1.66 barns, which yields a mean free path of 27 g cm^{-2}. Thus in an aluminum shield of 10 g cm^{-2} depth, about 30% of incident silicon ions will undergo fragmentation. If instead a water shield is used in the calculation, the predicted fraction of silicon ions undergoing fragmentation rises to about 49%. The differences in fragmentation in various materials are the basis on which hydrogenous shields were found by Wilson et al. (1995) to offer superior performance compared to heavier materials such as aluminum. The advantage arises because of the relatively large nuclear cross section per unit mass on hydrogen target nuclei.

The Z^2 dependence of dE/dx also means that relatively more heavy ions range out in a moderately thick shield than do protons or helium ions. However, the same physical effect can result in an increased dose, by slowing a heavy ion down significantly so its dE/dx (and hence LET) increase, provided it neither stops nor fragments in the shield.

Competing Effects

To summarize the preceding discussion, Table 2 provides a list of the physical mechanisms at work as an incident particle enters a shield and the possible outcomes related to these effects.

The probabilities of the different outcomes for each mechanism depend on the charge and energy distributions of the incident radiation, the composition of the shield, and in the case of dose equivalent, details of the quality factor used in the integration over the LET spectrum.

Space Radiation Shielding, Table 2 Important physical processes in space radiation shielding

Mechanism	Affects	Possible benefit	Possible detriment
Ionization energy loss	Charged particles	Low-energy particles are stopped in the shield	Particles are slowed but not stopped in shield, have larger LET after shield than before
Proton-nucleus collision	Protons	A small fraction of low-energy protons may stop in the shield due to energy lost in collisions	Production of secondary radiation causes increased dose behind shield
Nucleus-nucleus collision	Ions with $Z > 1$	Fragmentation into lower-Z ions results in decreased dose behind shield	Though dose is decreased after fragmentation, dose equivalent may increase

A manifestation of the competing effects can be seen in the Bragg curves (dose vs. depth) for heavy ion beams used in radiation therapy (Zeitlin 2012) and for radiation biology experiments (Zeitlin et al. 1998). For particular combinations of beam ion and energy, e.g., carbon at 290 MeV/nuc in water, dose versus depth curves may be flat or nearly so over many centimeters of depth, indicating that the competing effects of ionization energy loss and fragmentation balance each other. In other cases, e.g., for the 1 GeV/nuc ^{56}Fe beam used in many biology studies, dose falls monotonically with depth as fragmentation is the dominant physical process, until the depth at which the iron ions stop is reached; at that point, the curve turns up but never reaches the initial value, because so much of the initial beam has been fragmented before it can come to rest. At low energies, heavy ion Bragg curves may be monotonically increasing, as energy loss dominates over fragmentation.

Radiological Quantities in Detail

To evaluate the effectiveness of shielding in any particular exposure scenario, it is necessary to construct a quantitative framework that reflects the potential of the radiation field either outside or inside the shield to cause biological harm. The simplest approach is to consider the radiation dose, defined to be the energy deposited per unit mass at a given point in the field. Dose is a purely physical quantity, and while there is no doubt that shielding that reduces dose is valuable, it is well known in radiation biology that dose alone is insufficient to describe the biological effects of particles of various types. That is, for a given dose, biological effects may be very different depending on the type of particle that delivered the dose. Recognizing this fact, the ICRP has long defined LET-dependent quality factors for cancer induction, including the widely-used version denoted ICRP 60 (ICRP 1991). The ICRP 60 quality factor Q is defined to be a function solely of LET, i.e., Q(L). This is a useful approximation, as LET and its proxy lineal energy are measurable quantities, but in the NASA framework of risk assessment (Cucinotta et al. 2012), the LET dependence has been replaced by a Z^2/β^2 dependence that is more reflective of track structure. In the ICRP 60 definition, for LET below 10 keV/μm (i.e., low-LET radiation), Q is identically 1; between 10 and 100 keV/μm, Q rises according to $Q(L) = 0.32\ L - 2.2$, reaching a peak value of 30 at 100 keV/μm; and above 100 keV/μm, Q falls according to $Q(L) = 300/L^{1/2}$. This piecewise function was derived by evaluating a variety of radiobiology data with considerable scatter: that Q(L) is accordingly highly uncertain should be kept in mind.

The dose equivalent is often written as H, and is given by $H = \langle Q \rangle D$, where D is the dose and $\langle Q \rangle$ is the dose-weighted average quality factor. Because heavy ions have high LET, they have a strong effect on $\langle Q \rangle$. For instance, in unshielded free space, even though the flux of GCRs consists of 99% low-LET particles having Q of 1, $\langle Q \rangle$ is predicted to be between 6 and 7, depending on the state of solar modulation.

Assessment of Bulk Shielding Against GCRs

Knowledge of the space radiation environment, the physics of shielding against space radiation, and a radiological framework (dose and dose equivalent)

are the necessary pieces for assessing space radiation exposures. These pieces can be, and have been, assembled into various space radiation transport codes. An easy-to-use interface to a transport model, OLTARIS, has been provided to researchers by scientists at the NASA Langley Research Center (Singleterry 2011). Passive or "bulk" shielding as provided by the hull of a spacecraft, or by regolith in a buried habitat on the Moon or Mars, can readily be evaluated with OLTARIS for various space radiation environments.

Important calculations of GCR shielding were provided by Wilson et al. (1995). Using the state-of-the-art calculation tools, the authors showed that the dose equivalent from GCRs would be most reduced by a shield comprised of liquid hydrogen, while shields composed of heavier elements such as aluminum give only a very modest attenuation. The transport code provided by OLTARIS is an updated version (Slaba et al. 2010) of the HZETRN code (Shinn and Wilson 1992) used in the earlier calculations. OLTARIS also makes updated environment models available. It is instructive to revisit the earlier calculations with these new and improved tools. Rather than repeat the full set of shields, the calculations have been run for hydrogen and aluminum, in keeping with the original work. The GCR flux model developed by Matthiä et al. (2013) was chosen, for solar conditions corresponding to the 2001 maximum. Results for dose (left panel) and dose equivalent (right panel) are shown in Fig. 4. Remarkably, for the aluminum shield, the dose is greater at depths up to and including 100 g cm^{-2} than it is in the unshielded environment. This is due to the production of secondary particles in the shield, which outweighs the effects of heavy ion fragmentation. This result is in stark contrast to that for the pure hydrogen shield, which produces a steep decrease with depth over the first 10–20 g cm^{-2}, with the curve starting to level off at greater depths. There is comparatively more fragmentation of heavy ions and much less secondary production in the hydrogen shield.

Results for dose equivalent are in one sense similar to those for dose, in that the hydrogen shield clearly performs much better than the aluminum shield. However, in dose equivalent, the aluminum shield can be said to have a net benefit in that dose equivalent values at depth are less than in free space; this is not the case for dose. The apparently better performance in terms of dose equivalent is again due to heavy ion fragmentation. Even in dose equivalent, the curves level off or even rise slightly as depth increases beyond 50 g cm^{-2}. This shows that there is no benefit in going beyond this depth of shielding, and only marginal reductions in dose equivalent are seen in going from 20 to 50 g cm^{-2} in either material. These results are qualitatively very similar to those calculated in 1995 and also demonstrate that conclusions about shielding effectiveness may be sensitive to the biological response model, which in this case is represented by Q(L).

The value of $<Q>$ at a particular depth can be inferred from the ratio of dose equivalent to dose. This is an approximate indicator of the number of heavy ions that have survived traversal of the shield. At a depth of 20 g cm^{-2} of hydrogen shielding, $<Q>$ is 1.4, indicating that the heavy ions have largely been attenuated. The advantages of hydrogenous materials as heavy ion shields have been confirmed both in the laboratory using particle beams (Zeitlin et al. 2006) and using the CRaTER instrument in lunar orbit (Spence et al. 2010) to study GCR shielding by tissue-equivalent plastic (Zeitlin et al. 2013b).

While the preceding discussion suggests that pure hydrogen shields would enable safe interplanetary travel, it should be noted that at present, there is no workable design for such a spacecraft. Hydrogen for use as fuel, and in the form of water for the crew's use, may be abundant on such spacecraft, but hulls and cryogenic containment vessels, presumably quite massive and made of aluminum or other structural material, will still be needed. These will be the outer shell or shells and will compromise the overall shield performance. Furthermore, though a hydrogen shield would significantly attenuate the flux of high-LET primary GCRs, other sources of high-LET exposure would persist inside the shielding, notably secondary neutrons, and high-energy GCR protons that pass through the shield that would still create high-LET secondaries via proton-nucleus interactions in the body. The latter

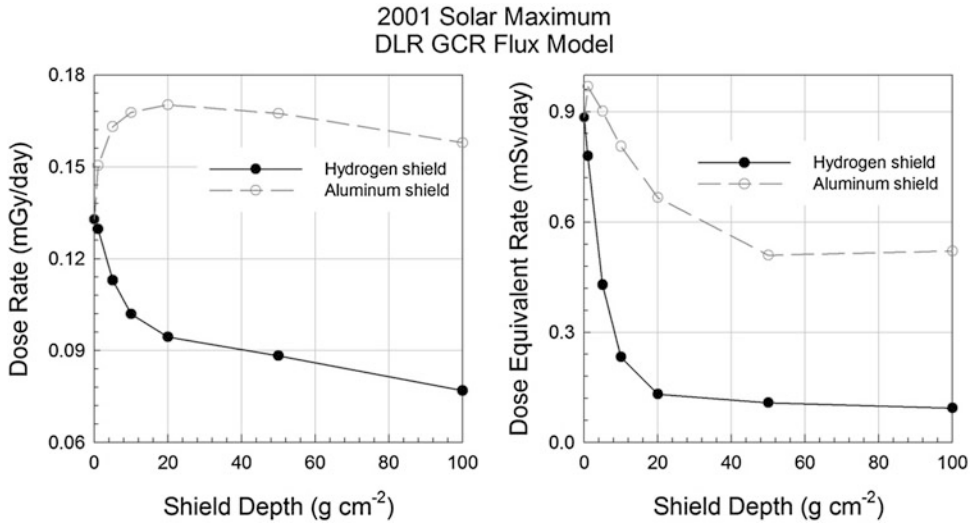

Space Radiation Shielding, Fig. 4 OLTARIS calculations of dose versus depth and dose equivalent versus depth for aluminum and hydrogen targets, for heliospheric conditions corresponding to the 2001 solar maximum

effect is not accounted for in the preceding calculations.

Assessment of Bulk Shielding Against SEPs

While practical depths of bulk shielding provide modest reductions in the GCR dose equivalent, the same depths are highly effective in reducing exposure to SEPs. The September 1989 SEP event was chosen. This event may have had the hardest energy spectrum of any event in the Space Age (Tylka and Dietrich 2009), so that it could represent the worst-case scenario. This spectrum can be invoked for transport calculations in OLTARIS, and Fig. 5 shows the results for dose equivalent versus depth for aluminum and hydrogen shields. These are "event-integrated" dose equivalents, that is, the accumulated totals over the full duration of the event. The sharp decrease with depth shows that, unlike GCRs, the large majority of SEPs are stopped. At 5 g cm^{-2} depth, the shields give reductions in dose equivalent of 4–5 orders of magnitude compared to unshielded space. Hydrogen is again more effective than aluminum, but even aluminum provides sufficient protection at 20 g cm^{-2} given the current exposure limit of 250 mSv to the blood-forming organs (Durante and Cucinotta 2011).

The effectiveness of bulk shielding against SEPs is a direct result of the fact that the large majority of accelerated particles have energies below 100 MeV/nuc. The range of a proton with this energy is about 4 cm, or 10 g cm^{-2}, in aluminum. Thus in many SEP events, virtually all of the incident particles can be stopped in a modest shield. There is still some production of secondaries that penetrate the shield, but as described in the preceding, this is far less probable at typical SEP energies than at typical GCR energies.

Active Shielding

Active approaches to space radiation shielding, that is, the use of powerful magnetic or electrostatic fields, or plasma "bubbles" surrounding a spacecraft, have been repeatedly proposed for more than 50 years (Levy 1961; Landis 1991; Calvelli et al. 2014; Bamford et al. 2014). However, little progress has been made toward their realization. Proposed active shielding concepts were thoroughly reviewed by NASA in 2005 (Adams et al. 2005), and shortly thereafter several important papers were published (Townsend 2005; Parker 2006; Spillantini et al. 2007) that also examined these concepts. All reviews reached generally pessimistic conclusions as to the viability of active shielding with regard to

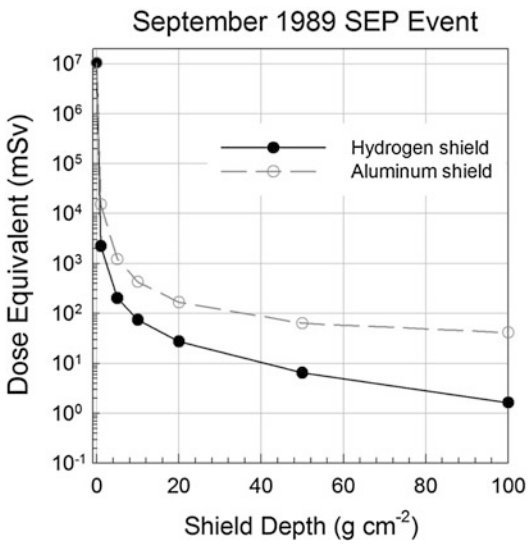

Space Radiation Shielding, Fig. 5 Calculated event-integrated dose equivalent values as functions of shielding depth for the large SEP event of September 1989. The OLTARIS code described in the text was used for the calculations. Both aluminum and hydrogen shields are effective against SEPs, but hydrogen is more effective, as is also the case for GCRs

protecting against GCRs. The situation is slightly more hopeful for protecting against SEPs, but the preceding discussion shows that passive shielding is generally adequate for that task. The interested reader is referred to these articles for detailed descriptions of the proposed shielding methods and the serious technological hurdles that remain before any type of active shielding is ready for spaceflight. Although these reviews are a decade old at the time of this writing, the underlying physics is obviously unchanged, and no enabling technological breakthroughs have been made in these areas.

Despite the many difficulties, work continues in the area of active shielding, with some apparent progress (Westover et al. 2014; Del Rosso 2015). But, as observed by Townsend (2005), active shields will require massive support structures and may require complex infrastructure to operate and maintain; the primary question is whether such shields offer improved protection against energetic particles compared to bulk shielding having the same total cost. Recent simulations that include support structures (Vuolo et al. 2015) indicate that secondary production significantly degrades the performance of a proposed toroidal magnetic shield, again raising doubts about viability. Comparisons of active and passive shields must also take into account the advantages of relatively lightweight hydrogen-rich passive shielding materials and of the propensity for high-energy protons to penetrate any shield and create high-LET energy depositions in tissue via nuclear interactions.

Brief summaries are given here of the concepts that underlie proposals to use confined magnetic fields and electrostatic fields to protect against space radiation.

Magnetic Shielding

A charged particle moving in a magnetic field experiences a vector force $\vec{F}$, given by $\vec{F} = q\left(\vec{v} \times \vec{B}\right)$ where q is the charge of the particle, $\vec{v}$ its velocity vector, and $\vec{B}$ the magnetic field vector. The force is exerted in the direction perpendicular to the plane formed by the velocity and magnetic field vectors. A charged particle's trajectory is therefore bent in a magnetic field, raising the possibility that a crewed spacecraft could be protected from SEPs and GCRs by strong magnetic fields that deflect incident charged particles away from inhabited areas of the craft. However, there are severe practical difficulties shielding against GCRs, stemming from the fact that many of them have high energies and therefore require very high field strengths to cause significant deflection. For example, as pointed out by Parker (2006), deflecting a proton with 2 GeV of kinetic energy in a space of a few meters requires a field strength of about 20 T, much higher than the fields attained with large superconducting magnets in experimental high-energy physics experiments such as those at the Large Hadron Collider. The mass and power consumption of such systems quickly become problematic, and in addition there are safety questions, as a huge amount of energy would be stored in a static field, release of which would be extremely dangerous in the event of a sudden magnet quench. Designs must also minimize the strength of fringe

fields in inhabited regions of a spacecraft, as the health effects of long-term occupation of high field regions are unknown but quite possibly detrimental.

The experience of the Alpha Magnetic Spectrometer (Barao 2004), a large particle detector attached to the ISS, may be instructive with regard to present capabilities. An advanced, cryogenically cooled superconducting magnet with field strength of 0.87 Tesla at its center was built (Blau et al. 2002) but was not flown. It was to be the first large superconducting magnet in space, but in 2010, it was replaced by a permanent magnet with roughly one-fifth the field strength. The change was necessitated by tests that showed the superconducting magnet ran warmer than expected, meaning it would deplete its supply of liquid helium more quickly than planned and consequently shorten the lifetime of the experiment. Of course this does not preclude successful deployment of future superconducting magnets, but it is an indicator that even with the most advanced technology presently available, such an undertaking still presents many challenges, even on a smaller scale than would be required to shield a crewed interplanetary spacecraft.

Electrostatic Shielding

Like magnetic shielding, electrostatic shielding can provide significant protection against the space radiation environment in principle. The basic idea of an electrostatic shield is to create a region of space outside a spacecraft with an intense electric field to deflect charged particles away from the crew. Perhaps the simplest such concept calls for two concentric conducting spheres with opposite, large static charges on them (Towsend 1984). The inner sphere would be the hull of the spacecraft, with crew inside, bearing a positive charge, while the outer sphere would be built specifically for the purpose of holding negative charge. The two spheres would in essence form a large capacitor with the field confined to the space between them. There are several problems with this approach. First, avoiding vacuum breakdown in this configuration requires that the conducting spheres be hundreds of meters in radius. Second, the arrangement requires extreme stability, i.e., the spheres must be held rigidly in place, requiring significant additional mass. Finally, the most severe problem with this concept is the huge electrostatic potential required to deflect high-energy, highly charged GCRs: this is on the order of 10^9 volts, roughly two orders of magnitude greater than is currently feasible. A far more sophisticated design has been put forward by Tripathi et al. (2008), making use of lightweight gossamer structures. Preliminary tests using scaled-down structures show some promise (Stiles et al. 2013), but new challenges emerged even in small-scale tests, and the required electrostatic potentials remain far beyond what is presently possible.

References

Adams JH et al (2005) Revolutionary concepts of radiation shielding for human exploration of space. NASA TM 213688

Agostinelli S et al (2003) GEANT4 – a simulation toolkit. Nucl Instr Meth A 506:250–303

Baade W, Zwicky F (1934) On super-novae. Proc Natl Acad Sci 20(5):254–259

Bamford RA et al (2014) An exploration of the effectiveness of artificial mini-magnetospheres as a potential solar storm shelter for long term human space missions. Acta Astronaut 105(2):385–394

Barao F (2004) AMS – alpha magnetic spectrometer on the international space station. Nucl Instrum Methods Phys Res, Sect A 535(1):134–138

Berger MJ (1992) ESTAR, PSTAR and ASTAR: computer codes for calculating stopping power and range tables for electrons, protons and helium ions. National Institute of Standards and Technology report, NISTIR 4999

Bethe H (1930) Zur theorie des durchgangs schneller korpuskularstrahlen durch materie. Ann Phys 397(3):325–400

Blasi P (2013) The origin of galactic cosmic rays. Astron Astrophys Rev 21(1):1–73

Blau B et al (2002) The superconducting magnet system of AMS-02-a particle physics detector to be operated on the international space station. Appl Supercond IEEE Trans 12(1):349–352

Bradt HL, Peters B (1950) The heavy nuclei of the primary cosmic radiation. Phys Rev 77(1):54

Brenner DJ et al (2003) Cancer risks attributable to low doses of ionizing radiation: assessing what we really know. Proc Natl Acad Sci 100(24):13761–13766

Calvelli V, Farinon S, Burger, WJ, Battiston R (2014) Space radiation superconducting shields. In Journal of Physics: Conference Series 507(3), p. 032033). IOP Publishing

Charbonneau P (2014) Solar dynamo theory. Annu Rev Astron Astrophys 52:251–290
Cliver EW, Dietrich WF (2013) The 1859 space weather event revisited: limits of extreme activity. J Space Weather Space Clim 3:A31
Cucinotta (2015) A new approach to reduce uncertainties in space radiation cancer risk predictions. PLoS One. https://doi.org/10.1371/journal.pone.0120717
Cucinotta FA et al (1991) Biological effectiveness of high-energy protons: target fragmentation. Radiat Res 127(2):130–137
Cucinotta FA, Kim MHY, Ren L (2006) Evaluating shielding effectiveness for reducing space radiation cancer risks. Radiat Meas 41(9):1173–1185
Cucinotta FA, Kim MHY, Chappell L (2012) Space radiation cancer risk projections and uncertainties- 2012. NASA TP 2013-217375
Del Rosso A (2015) A superconducting shield to protect astronauts. CERN Bull. Issue no 32–33/2015, 3 August 2015
Detmold W (2015) Nuclear physics from lattice QCD. Lattice QCD for nuclear physics. Springer International Publishing, Berlin. pp 153–194
Durante M, Cucinotta FA (2011) Physical basis of radiation protection in space travel. Rev Mod Phys 83(4):1245
Hathaway DH (2010) The solar cycle. Living Rev Solar Phys **7**:1. http://www.livingreviews.org/lrsp-2010-1. Cited on 15 Aug 2015
Hess VF (1913) Über den Ursprung der durchdringenden Strahlung. Z Phys 14:610
International Commission on Radiological Protection (1991) ICRP publication 60: 1990 recommendations of the international commission on radiological protection. no. 60. Elsevier Health Sciences, Oxford
Landis GA (1991) Magnetic radiation shielding- an idea whose time has returned? In: Space manufacturing 8 – Energy and materials from space; Proceedings of the 10th Princeton/AIAA/SSI Conference, Princeton, NJ, (A92-17751 05-12). Washington, DC, American Institute of Aeronautics and Astronautics, p. 383–386.
Levy RH (1961) Radiation shielding of space vehicles by means of superconducting coils. Structure 1:2
Matthiä D et al (2013) A ready-to-use galactic cosmic ray model. Adv Space Res 51(3):329–338
Mewaldt RA et al. (2005) Solar-particle energy spectra during the large events of October-November 2003 and January 2005. International cosmic ray conference, vol. 1
Moyers MF, Saganti PB, Nelson GA (2006) EVA space suit proton and electron threshold energy measurements by XCT and range shifting. Radiat Meas 41(9):1216–1226
Niita K et al (2006) PHITS – a particle and heavy ion transport code system. Radiat Meas 41(9):1080–1090
Nymmik RA, Panasyuk MI, Suslov AA (1996) Galactic cosmic ray flux simulation and prediction. Adv Space Res 17(2):19–30
O'Neill PM, Golge S, Slaba, TC (2015) Badhwar – O'Neill 2014 galactic cosmic ray flux model. NASA/TP 218569
Oh JH et al (2015) Study on radiation production in the charge stripping section of the RISP linear accelerator. J Korean Phys Soc 66(3):432–438
Olive KA et al (Particle Data Group) (2014) Review of particle physics. Chin Phys C 38:090001
Paganetti H (2002) Nuclear interactions in proton therapy: dose and relative biological effect distributions originating from primary and secondary particles. Phys Med Biol 47(5):747
Parker EN (2006) Shielding space explorers from cosmic rays. Space Weather 3:8
Reames D (1999) Solar energetic particles: is there time to hide? Radiat Meas 30(3):297–308
Reitz G et al (2005) Space radiation measurements on-board ISS – the DOSMAP experiment. Radiat Prot Dosim 116(1–4):374–379
Ronningen RM, Remec I, Heilbronn LH (2013) Benchmarking heavy ion transport codes FLUKA, HETC-HEDS MARS15, MCNPX, and PHITS. No. DOE/ER/41548. Michigan State University, East Lansing, MI (US)
Schwabe H (1844) Sonnen-Beobachtungen im Jahre 1843. Astron Nachr 21(495):233–236
Shinn JL, Wilson JW (1992) An efficient heavy ion transport code: HZETRN. NASA TP-3147
Sihver L et al (2007) Recent developments and benchmarking of the PHITS code. Adv Space Res 40(9):1320–1331
Singleterry RC et al (2011) OLTARIS: on-line tool for the assessment of radiation in space. Acta Astronaut 68(7):1086–1097
Slaba TC, Blattnig SR, Badavi FF (2010) Faster and more accurate transport procedures for HZETRN. J Comput Phys 229(24):9397–9417
Smart DF, Shea MA, McCracken KG (2006) The carrington event: possible solar proton intensity – time profile. Adv Space Res 38(2):215–225
Spence HE et al (2010) CRaTER: the cosmic ray telescope for the effects of radiation experiment on the lunar reconnaissance orbiter mission. Space Sci Rev 150(1–4):243–284
Spillantini P et al (2007) Shielding from cosmic radiation for interplanetary missions: active and passive methods. Radiat Meas 42(1):14–23
Stephens DL, Townsend LW, Hoff JL (2005) Interplanetary crew dose estimates for worst case solar particle events based on historical data for the carrington flare of 1859. Acta Astronaut 56(9):969–974
Stiles LA et al (2013) Electrostatically inflated gossamer space structure voltage requirements due to orbital perturbations. Acta Astronaut 84:109–121
Stone EC et al (2013) Voyager 1 observes low-energy galactic cosmic rays in a region depleted of heliospheric ions. Science 341(6142):150–153

Townsend LW (2005) Critical analysis of active shielding methods for space radiation protection. Aerospace conference, 2005 IEEE

Townsend LW, and Wilson JW (1986) Energy-dependent parameterization of heavy-ion absorption cross sections. Radiation research 106(3):283–287

Townsend LW et al (2006) The carrington event: possible doses to crews in space from a comparable event. Adv Space Res 38(2):226–231

Towsend LW (1984) Galactic heavy-ion shielding using electrostatic fields. NASA Technical Memorandum 86265

Tripathi RK, Wilson JW, Youngquist RC (2008) Electrostatic space radiation shielding. Adv Space Res 42(6):1043–1049

Tylka AJ, Dietrich WF (1999) IMP-8 observations of the spectra, composition, and variability of solar heavy ions at high energies relevant to manned space missions. Radiat Meas 30(3):345–359

Tylka AJ, Dietrich WF (2009) A new and comprehensive analysis of proton spectra in ground-level enhanced (GLE) solar particle events. In: Proceedings of the 31st ICRC, Lodz, pp 7–15

Vuolo M et al (2015) Monte Carlo simulations for the space radiation superconducting shield project (SR2S). Life Sci Space Res 8:22–29

Westover SC et al. (2014) Magnet architectures and active radiation shielding study (MAARS), final report for NASA innovative advanced concepts phase I. NASA TP-2014-217390

Wilson JW et al (1995) Issues in space radiation protection: galactic cosmic rays. Health Phys 68(1):50–58

Wolff EW et al (2012) The carrington event not observed in most ice core nitrate records. Geophys Res Lett 39(8): L08503

Zeitlin C, Heilbronn L, Miller J (1998) Detailed characterization of the 1087 MeV/nucleon iron-56 beam used for radiobiology at the alternating gradient synchrotron. Radiation research 149(6):560–569

Zeitlin C (2012) Physical interactions of charged particles for radiotherapy and space applications. Health Phys 103(5):540–546

Zeitlin C et al (2006) Measurements of materials shielding properties with 1 GeV/nuc ^{56}Fe. Nucl Instrum Methods Phys Res Sect B: Beam Interact Mater Atoms 252(2):308–318

Zeitlin C et al (2013a) Measurements of energetic particle radiation in transit to Mars on the Mars Science Laboratory. Science 340(6136):1080–1084

Zeitlin C et al (2013b) Measurements of galactic cosmic ray shielding with the CRaTER instrument. Space Weather 11(5):284–296